

LPV Modeling for Control Scheme Design of a Compound Helicopter



Bowen Nie, Zhiyin Huang, Long He, Liangquan Wang, and Olivier Sename

Abstract The compound helicopter is able to reach speeds that significantly surpass the conventional counterpart. However, the compounding of lift and thrust always results in more complicated aerodynamic and control issues than a conventional helicopter. Therefore, it is important to model and evaluate the flight dynamics in the early design phase of a compound configuration. The aim of this paper is to develop a Linear-Parameter-Varying (LPV) model of a compound helicopter and investigate the trim, stability and control characteristics. A series of discrete linear state-space models and trim data are obtained from the nonlinear mathematic model, and then interpolated for construction of a LPV model with respect to two scheduling parameters. Lastly, the LPV model is augmented with control scheme to perform flight simulation covering the speed envelope.

Keywords Compound helicopter · LPV modeling · Control scheme · Flight simulation

1 Introduction

The maximum flight speed of conventional helicopter is restricted by adverse aerodynamic effects of stall on the retreating blades and compressibility on the advancing blades of the main rotor [1]. Compounding is a promising solution to increase

B. Nie · Z. Huang (✉) · L. He · L. Wang
Key Laboratory of Rotor Aerodynamics, China Aerodynamics Research and Development Center,
Mianyang 621000, China
e-mail: huangzhiyin@cardc.cn

B. Nie
e-mail: niebowen@cardc.cn

O. Sename
GIPSA-Lab, Université Grenoble Alpes, CNRS, Grenoble INP, 3800 Grenoble, France

© The Author(s), under exclusive license to Springer Nature Singapore Pte Ltd. 2024
G. L. Conte and O. Sename (eds.), *Proceedings of the 11th International Conference on Mechatronics and Control Engineering*, Lecture Notes in Mechanical Engineering,
https://doi.org/10.1007/978-981-99-6523-6_4

the maximum flight speed of the helicopter. In recent years, helicopter manufacturers, such as Sikorsky and Airbus Helicopters (AH), are exploring and testing the compounding prototypes for future civil and military applications [2].

In practice, both lift and thrust compounding are required to increase the maximum speed of the helicopter. Take the AH X3 as example, the lift compounding is realized with wings to offload the main rotor at high speed, the thrust compounding is equipped with propellers to replace the tail-rotor at low speed and provide propulsive force at high speed. Consequently, the compound helicopter encounters inherent design and modeling challenges, in terms of complicated rotor dynamics, aerodynamic interactions, and redundant controls. To improve the design of compounding configuration at the initial design phase, it is essential to assess the stability, controllability and performance with a full flight-envelope high-fidelity flight dynamic model. Recent studies have performed various approaches to model the flight dynamics of compound helicopter. The practical modeling techniques are composed of low-fidelity models [3, 4] with limited components or neglected mechanics, comprehensive models [5] with multidisciplinary high-fidelity tool chain, and linearized models around the trimmed condition of steady flight [6]. However, the models mentioned in the foregoing sentence are either low-fidelity or sophisticated.

The approach of LPV modeling is adequate to trade off the fidelity and complexity of mathematical model for compound helicopter. In this technique, a set of linear state-space models are obtained by trimming and linearizing the nonlinear high-fidelity model at discrete flight conditions, and then meshed together to form a continuous and time-varying mathematical model covering the entire flight envelope. Application of the LPV framework to fixed wing aircrafts [7, 8], helicopters [9, 10] and tiltrotor aircrafts [11] can be found in literature. However, a rear number of studies have been carried out for compound helicopters. The aim of this paper is to develop a LPV model for compound helicopter representative of AH X3 with two varying parameters: velocity V and rotor speed Ω . The resulting LPV model can be utilized not only for the purpose of full-envelope simulation but also for the Stability and Control Augmentation System (SCAS) design.

The paper is organized as follow. First, a brief theoretical background of LPV and quasi-Linear-Parameter-Varying (qLPV) is introduced. Second, a nonlinear mathematical dynamic model of the studied compound helicopter is presented. Next, a LPV model is constructed by scheduling the state-space models and corresponding trim values for a set of grid points. Lastly, a SCAS is designed and applied to the LPV model for closed-loop simulation covering the speed envelope.

2 Theoretical Background

LPV systems are linear state-space models that depend on a time varying parameter vector $\rho(t)$. Namely, a collection of linear state-space models and the corresponding trim data, obtained at a set of discrete equilibrium points, can be combined into lookup tables and interpolated as function of the scheduling parameters [12]. As a

result, a LPV system is defined as following:

$$\dot{X}(t) = A(\rho(t))(X(t) - X_0(\rho(t))) + B(\rho(t))(U(t) - U_0(\rho(t))) \quad (1)$$

$$Y(t) = C(\rho(t))(X(t) - X_0(\rho(t))) + D(\rho(t))(U(t) - U_0(\rho(t))) \quad (2)$$

where X , U and Y are the state, input and output vectors, X_0 , U_0 and Y_0 are the operating point state, input and output vectors, respectively.

A qLPV system is a particular case of LPV system, when a subset of scheduling parameter is also state of system. Namely, the state vector $X = [Z, W]^T$ is composed of scheduling states $Z \subset \rho(t)$ and non-scheduling states $W \not\subset \rho(t)$. Consequently, the LPV system of Eq. (1) can be rewritten as:

$$\begin{bmatrix} \dot{Z} \\ \dot{W} \end{bmatrix} = \begin{bmatrix} A_{11}(\rho) & A_{12}(\rho) \\ A_{21}(\rho) & A_{22}(\rho) \end{bmatrix} \begin{bmatrix} Z - Z_0(\rho) \\ W - W_0(\rho) \end{bmatrix} + \begin{bmatrix} B_1(\rho) \\ B_2(\rho) \end{bmatrix} [U - U_0(\rho)] \quad (3)$$

Since Z is used in the scheduling parameter function $\rho(t)$ and also state of the system, $Z - Z_0(\rho) = 0$ is always true. Therefore, Eq. (3) can be simplified as following:

$$\begin{bmatrix} \dot{Z} \\ \dot{W} \end{bmatrix} = \begin{bmatrix} A_{11}(\rho) & A_{12}(\rho) \\ A_{21}(\rho) & A_{22}(\rho) \end{bmatrix} \begin{bmatrix} 0 \\ W - W_0(\rho) \end{bmatrix} + \begin{bmatrix} B_1(\rho) \\ B_2(\rho) \end{bmatrix} [U - U_0(\rho)] \quad (4)$$

However, the contributions of scheduling states to \dot{Z} can be reserved implicitly through the variation of trim states and inputs as described in reference [13].

3 Compound Helicopter Mechanics

3.1 Hybrid Compounding Configuration

The studied helicopter employs hybrid compounding with both lift and thrust. Lift is generated by the main rotor and a jointed box wing, and thrust is provided simultaneously by the main rotor and a pair of lateral propellers mounted on the wing tips. Since auxiliary lift and thrust can be obtained at high speed, the hybrid compounding configuration is expected to reach a potential flight speed of $V = 68$ m/s.

Regarding the control surfaces of the studied compound helicopter, a mean collective pitch P_a of the propellers is responsible for the thrust, while a differential collective pitch P_d of the propellers is required to counteracts the anti-torque of the main rotor and addresses the yaw damping. In addition, an H-stabilizer helps to provide the horizontal, vertical static stability and rudder δ_r . Besides, there are three control

surfaces of the main rotor including the collective θ_0 , longitudinal cyclic pitch (B_1) and lateral cyclic pitch (A_1).

3.2 Nonlinear Dynamic Equations

To develop the nonlinear flight dynamic model, a summarization of the forces F^B and moments M^B with respect to the center of gravity in the body frame is required.

$$\begin{pmatrix} mI_3 & 0 \\ 0 & J \end{pmatrix} \begin{pmatrix} \dot{\vec{v}}^B \\ \dot{\vec{\omega}}^B \end{pmatrix} + \begin{pmatrix} \vec{\omega}^B \times m \vec{v}^B \\ \vec{\omega}^B \times J \vec{\omega}^B \end{pmatrix} = \begin{pmatrix} F^B \\ M^B \end{pmatrix} \quad (5)$$

where m is the mass, J is the inertia tensor, $\vec{v}^B = [u, v, w]^T$ and $\vec{\omega}^B = [p, q, r]^T$ are the translational and angular speed in the body-fixed frame, respectively.

As the compound helicopter is composed of several subsystems, the forces and moments can be decomposed as following:

$$\begin{cases} F^B = F_g + F_r + F_p + F_f + F_w + F_s + F_t \\ M^B = M_r + M_p + M_f + M_w + M_s + M_t \end{cases} \quad (6)$$

In Eq. (6), the subscripts of g, r, p, f, w, s and t denote the gravity, rotor, propeller, fuselage, wing, stabilizer and vertical tail, respectively.

To account for the nonlinear aerodynamics and rotor periodicity, an ‘individual blade model’ is developed for the main rotor and propellers using the approach described in reference [14]. Aerodynamic loads of the fuselage, wing and fins are obtained by a series of lookup tables and interpolations with the experimental data. Furthermore, dynamic inflow model and a rotor-speed governor model are also integrated to the nonlinear compound helicopter dynamics as described in reference [15, 16].

From a control point of view, the entire compound helicopter dynamics take the nonlinear form as:

$$\dot{\vec{x}} = f(\vec{x}, \vec{u}) \quad (7)$$

where $\vec{x} = [\Delta u, \Delta v, \Delta w, \Delta p, \Delta q, \Delta r, \Delta \phi, \Delta \theta, \Delta \psi]^T$ is the perturbation state vector composed of six rigid body speeds and three Euler angles (ϕ, θ, ψ), $\vec{u} = [\Delta A_1, \Delta B_1, \Delta P_d, \Delta \theta_0, \Delta P_a, \Delta \delta_r]$ is the perturbation control vector.

4 LPV Modelling Step

4.1 State-Space Point Models for the Compound Helicopter

In this paper, a LPV model is developed for a compound helicopter using two scheduling parameters: velocity V and rotor speed Ω . Velocity is selected as a scheduling parameter to capture the changing dynamics, such that the entire speed envelope can be covered. Rotor speed is chosen as an additional scheduling parameter to account for the dynamics induced by the rotor speed, which should be slow down to offload the main rotor as shown in Fig. 1.

The final choice of the scheduling parameters is given in Table 1. According to the two-dimensional scheduling network, there are 16 grid points. A collection of linear state-space models and the corresponding trim data is then generated for all the grid points. The resulting state-space models take the form of:

$$\sum_i = \begin{cases} \dot{\vec{x}} = A_i \vec{x} + B_i \vec{u} \\ \vec{y} = C_i \vec{x} + D_i \vec{u} \end{cases} \quad i = 1, 2, \dots, 16 \quad (8)$$

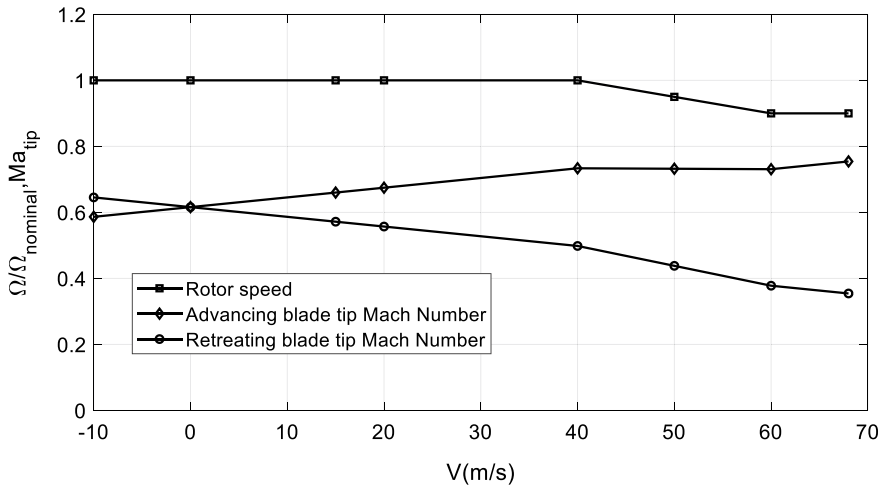


Fig. 1 Variation of rotor speed for the compound helicopter

Table 1 Scheduling parameters

Parameter	Values	Unit
Velocity V	[-10, 0, 15, 20, 40, 50, 60, 68]	m/s
Rotor speed Ω	[900, 1000]	rpm

where \vec{x} and \vec{u} are the same state and input vectors as Eq. (7), and $\vec{y} = \vec{x}$ is the output vector for sensor feedback.

4.2 LPV Model Structure for the Compound Helicopter

A block diagram schematic of the LPV model is shown in Fig. 2. Note that the aforementioned state-space point models are scheduled with $\rho = [V, \Omega]$, and then model meshing is implemented through lookup tables and interpolations. First, the lookup tables of trim control inputs, trim states and stability & control derivatives are generated as function of the scheduling parameters. Then, the interpolated trim control and trim states are subtracted from the current values to obtain the perturbations. Lastly, the control and state perturbations are multiplied with the interpolated control and stability matrices to calculate the state accelerations, which will be further integrated to obtain the current states.

Figure 3 presents an example for comparison of the trim values between the LPV model and the linear point models in terms of the pitch angle θ , rotor collective θ_0 and differential propeller collective P_d , which are captured off the grid nodes listed in Table 1. It is noted that the gain-scheduling LPV trim values show a good match with the linear point models across the flight speed envelope. As the flight speed increases, the wing offloads the main rotor and the vertical tail offloads the antitorque gradually. It is reasonable that the required trim values of θ , θ_0 and P_d decrease at high flight speed. This validates the LPV model, which captures the nonlinear characteristics of the compound helicopter.

Moreover, the modal characteristics of LPV model are calculated over the flight speed range -10 to 68 m/s at increments of 1 m/s, and compared with that of the linear point models off the grid points. It is observed that modal characteristics of the two models agree well with each other. This validates the LPV model, which captures the modal characteristics of the compound helicopter.

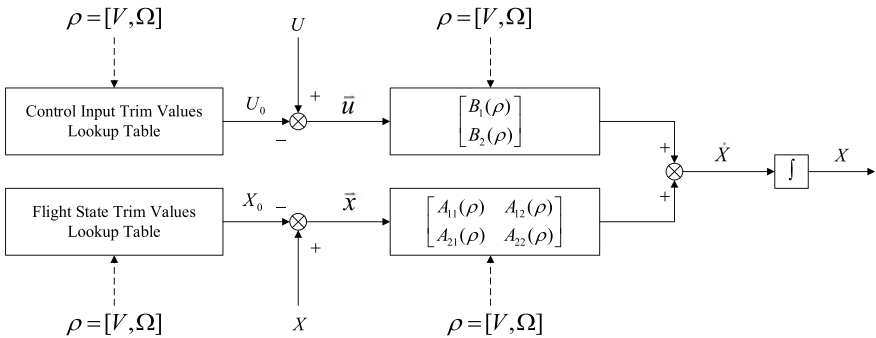


Fig. 2 LPV model structure for the compound helicopter

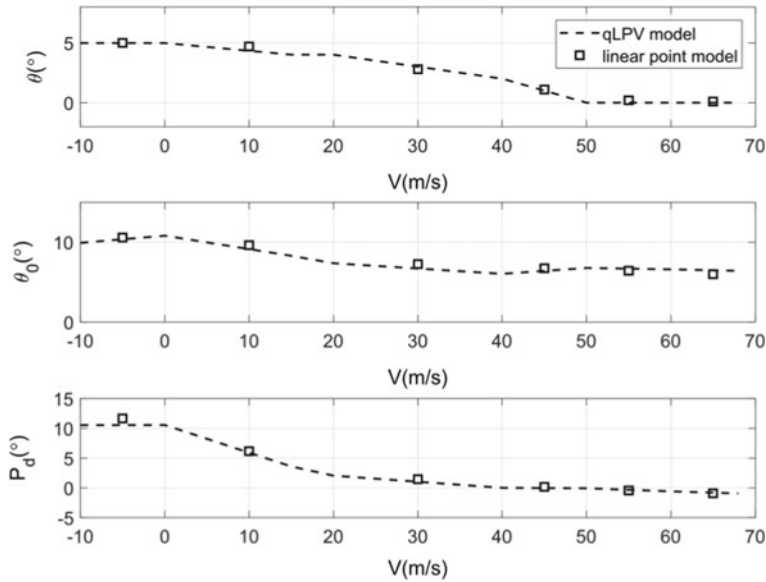


Fig. 3 Trim results of the nonlinear and LPV model

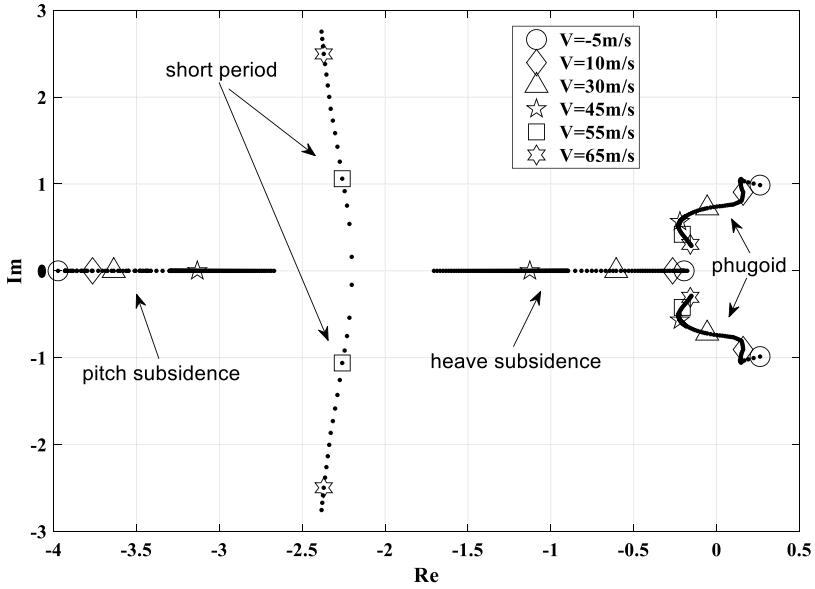
Figure 4a shows the longitudinal modes of the compound helicopter, including the phugoid, short period, pitch subsidence and heave subsidence. As can be seen, the pitch and heave subsidence modes combine to form short period mode as the flight speed increases. To be mentioned is that the phugoid mode is unstable at low speed while the damping of short period mode decreases at high flight speed. The lateral and directional modes are demonstrated in Fig. 4b. Similar to a conventional helicopter, the dutch roll mode is unstable at hover. As the speed increases, the dutch roll mode becomes stable. However, the damping of dutch roll mode decreases at high speed.

To conclude, it can be inferred that a SCAS is required to stabilize and control the compound helicopter over the speed envelope.

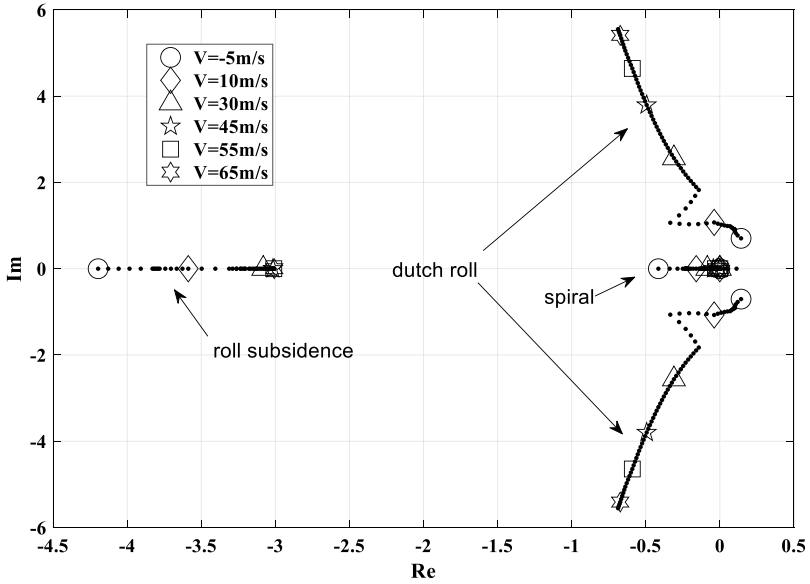
5 Simulation of LPV Model

5.1 Stability and Control Augmentation Scheme

To improve the stability and performance of the compound helicopter, a SCAS is designed based on the linear point models and then applied to augment the LPV model. The proposed SCAS scheme is presented in Fig. 5, which is composed of the longitudinal and lateral & directional channels.



(a) Longitudinal modal characteristics of the compound helicopter.



(b) Lateral and directional modal characteristics of the compound helicopter.

Fig. 4 Modal characteristics of the compound helicopter

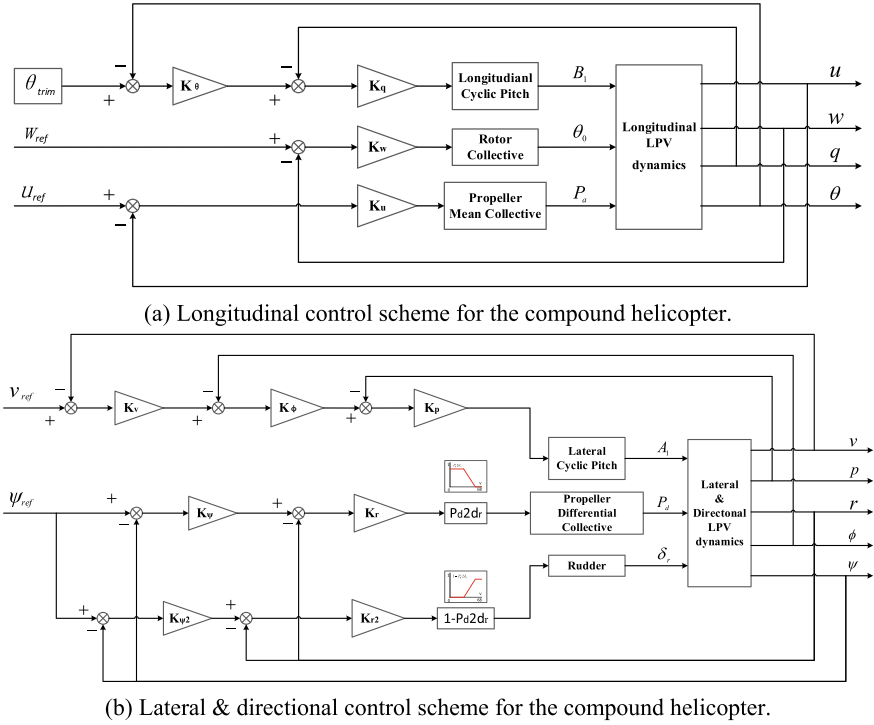


Fig. 5 Stability and control scheme for the compound helicopter

As demonstrated in Fig. 5a, the pitch rate feedback is introduced to improve the pitch damping, while the feedback loops of pitch angle, forward speed and heave speed are employed to track the references, respectively. Since the forward speed can be driven through the mean collective of the propellers, the forward speed is decoupled with the pitch attitude, and the trim values of pitch angle are selected as the reference. Furthermore, the feedback gains and θ_{trim} are scheduled to the flight speed.

The lateral & directional control scheme is shown in Fig. 5b. The roll rate, roll angle and lateral speed are cascaded to track the reference of lateral speed, while the yaw damping and yaw angle tracking loops are allocated to the differential propeller collective and the rudder, simultaneously. Actually, the commands of P_d and δ_r are scaled with two nondimensional factors, which are scheduled with the flight speed in the section of 0–1.

5.2 Closed-Loop Flight Simulation

The SCAS along with the LPV model are implemented for closed-loop simulation of the compound helicopter. A flight scenario covering the speed envelope is performed to validate the designed LPV model and control scheme. The scenario involves vertical take-off, hover, acceleration, high-speed cruise and deceleration as shown in Fig. 6.

The longitudinal time history is presented in Fig. 6a. One can see that the forward and heave speeds track the references well, and the forward speed covers the range from 0 to 68 m/s. Following the variation of forward speed, the reference value of pitch angle is automatically scheduled. Though notable tracking error is observed for pitch angle, the pitch angle is kept in the acceptable range of about 3° – 6° . Moreover, clip steps are found in the curve of the mean propeller collective at the time of about 50, 100, 120 and 170 s. This is caused by the variation of forward speed reference for accelerating or decelerating.

The lateral and directional time history is presented in Fig. 6b. Obviously, the roll and yaw attitudes are well damped and always kept around zero, though acceptable tracking errors are induced by the nonlinearity and coupling. To verify the feasibility of directional surface allocation, the mean and differential collective of the propellers are transformed to the collective of the left P_L and right P_R propeller. As is shown, both P_L and P_R locate in the available section of -15° to $+40^{\circ}$.

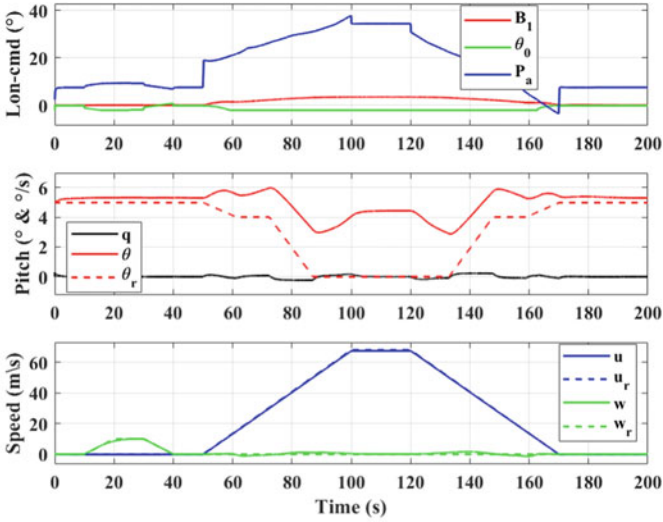
In summary, the time history reveals that the LPV model is adequate to capture the dynamics of the compound helicopter and the designed SCAS is effective to stabilize and control the compound helicopter throughout the speed envelope.

6 Conclusion

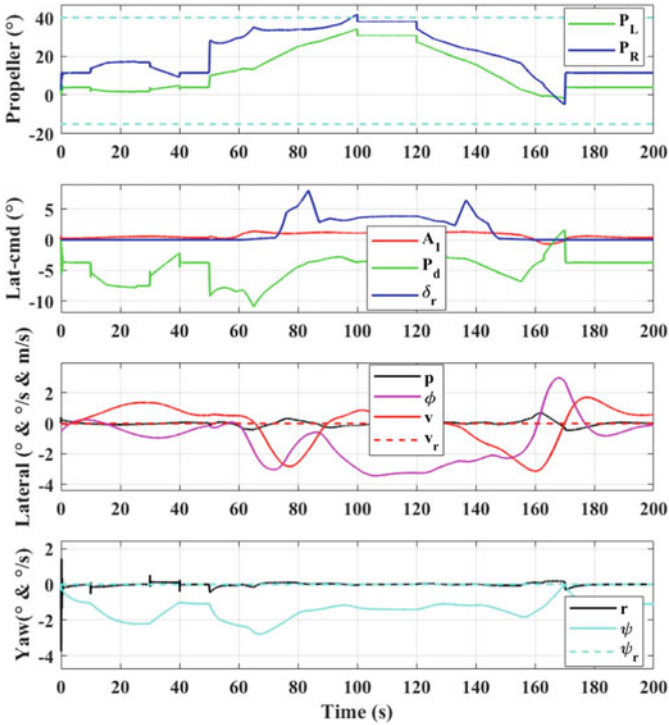
This paper presented the development of LPV model for a compound helicopter to trade off the fidelity and complexity. The state-space models and the corresponding trim values are scheduled with respect to the varying parameters of velocity and rotor speed. The implemented LPV model agrees well with the nonlinear dynamic model in terms of trim value and modal characteristics both on and off the scheduling grid points.

A SCAS is designed and applied to the LPV model for closed-loop flight simulation. A scenario involving vertical take-off, hover, acceleration, cruise and deceleration is performed to validate the dynamics and control scheme. The time history of flight simulation across the flight speed envelope reveals that the LPV model is adequate to capture the nonlinear dynamic characteristics of the compound helicopter, and the designed SCAS is effective to stabilize and control the compound helicopter.

In the future, research focus will be placed on implementing the LPV model and SCAS in experimental setup for further validation and improvement.



(a) Longitudinal time history.



(b) Lateral & directional time history.

Fig. 6 Time history of the flight simulation over the speed envelope

References

1. Filippone A (2006) Flight performance of fixed and rotary wing aircraft, CA
2. Hrlc C et al (2020) Compound helicopter X in high-speed flight: correlation of simulation and flight test. *J Am Helicopter Soc.* 66(1)
3. Lienard C, Salah el Din I, Renaud T, Fukari R (2018) RACER high-speed demonstrator: rotor and rotor-head wake interactions with tail unit. In: American helicopter society 74th annual forum
4. Stokkermans T, Voskuijl M, Veldhuis L, Soemarwoto B, Fukari R, Eglin P (2018) Aerodynamic installation effects of lateral rotors on a novel compound helicopter configuration. In: American helicopter society 74th annual forum
5. Thiemeier J et al (2020) Aerodynamics and flight mechanics analysis of Airbus Helicopters' compound helicopter RACER in hover under crosswind conditions. *CEAS Aeronaut J* 11(1):49–66
6. Panza S et al (2019) QLPV modelling of helicopter dynamics. *IFAC-PapersOnLine* 52(28):82–87
7. Tobias EL, Tischler MB (2016) A model stitching architecture for continuous full flight-envelope simulation of fixed-wing aircraft and rotorcraft from discrete-point linear models. U.S. Army AMRDEC SR RDMR-AF-16-01
8. Berger T, Tischler MB, Cotting MC, Gray WR (2020) Identification of a full-envelope Learjet-25 simulation model using a stitching architecture. *J Guide Control Dyn.* <https://doi.org/10.2514/1.G005094>
9. Zivan L, Tischler MB (2010) Development of a full flight envelope helicopter simulation using system identification. *J Am Helicopter Soc* 55(2):22003. <https://doi.org/10.4050/JAHS.55.022003>
10. Berger T, Juhasz O, Lopez MJS, Tischler MB, Horn JF (2020) Modeling and control of lift offset coaxial and tiltrotor rotorcraft. *CEAS Aeronaut J* 11(1):191. <https://doi.org/10.1007/s13272-019-00414-0>
11. Nabi HN, Visser CCD, Pavel MD et al (2021) Development of a quasi-linear parameter varying model for a tiltrotor aircraft. *CEAS Aeronaut J* 12:879–894 (2021). <https://doi.org/10.1007/s13272-021-00539-1>
12. Marcos A, Balas GJ (2007) Development of linear-parameter-varying models for aircraft. *J Guidance Control Dyn* 27(2):218–228
13. Tischler MB (2012) Aircraft and rotorcraft system identification: engineering methods with flight test examples, 2nd edn. American Institute of Aeronautics and Astronautics Inc., Reston, VA
14. Rutherford S (1997) Simulation techniques for the study of the maneuvering of advanced rotorcraft configurations, Ph.D. thesis. University of Glasgow, UK
15. Ferguson K, Thomson D (2016) Examining the stability derivatives of a compound helicopter. *Aeronaut J* 121(1235):1–20. <https://doi.org/10.1017/aer.2016.101>
16. Li et al (2010) A mathematical model for helicopter comprehensive analysis—ScienceDirect. *Chin J Aeronaut* 23(3):320–326